INNSPUB

Journal of Biodiversity and Environmental Sciences | JBES
ISSN: 2220-6663 (Print); 2222-3045 (Online)
Website: https://www.innspub.net
E-mail contact: info@innspub.net
Vol. 28, Issue: 2, p. 85-98, 2026

RESEARCH PAPER OPEN ACCESS

Using chitosan made from modified chitosan (Crab shells) for dye adsorption, equilibrium, kinetic, and response surface methods

M. Priyanga[1], V. Gomathi Priya[3], P. Bhuvaneswari[2], T. Shanmuga Vadivu[2], S. Viswanathan[3], G. Annadurai[1], R. Soranam[*1]

[1]*Sri Paramakalyani Centre of Excellence in Environmental Sciences, Manonmaniam Sundaranar University, Alwarkurichi, Tamil Nadu, India*

[2]*JP College of Arts and Science, Department of Chemistry, College Road, Agarakattu, Ayikudi, Tamil Nadu, India*

[3]*Post Graduate & Research Centre of Microbiology, Sri Paramakalyani College, Manonmaniam Sundaranar University, Alwarkurichi, India*

Key words: Crab shells, Chitosan, Methylene blue, Adsorption studies, Equilibrium studies

Received: 27 January, 2026 **Accepted:** 04 February, 2026 **Published:** 09 February, 2026

DOI: https://dx.doi.org/10.12692/jbes/28.2.85-98

ABSTRACT

Adsorption techniques based on the use of natural polymers, such as non-toxic chitosan, which is made from leftover crab shells by demineralization (acid treatment) and deproteinization (alkaline treatment), have drawn more attention in recent years. The most popular method for advanced wastewater treatment is adsorption. Because of its many functional uses, chitosan is frequently employed as an efficient biomaterial in the field of adsorption. Chitosan's hydroxyl (-OH) and amine ($-NH_2$) groups make it one of the most appropriate and adaptable adsorbents. By adding more functions to its fundamental structure, chitosan adsorption capability and selectivity can be further enhanced. While the Langmuir, Freundlich Isotherms study and kinetics investigations demonstrated that the adsorption process was suited by pseudo-first-order and second order for dye, the results from isotherm models demonstrated that the adsorption of dye on chitosan corresponded well with the Freundlich model. These three distinct factors influencing methylene blue adsorption performance were chosen for modelling and optimization procedures utilizing response surface methods in a central rotating composite design. A second-degree polynomial equation was used to predict the percentage of methylene blue elimination by chitosan made from crab shells. With an $R^2 = 0.9934$ and a Radj = 0.9849, the proposed model was valid and accurately described the phenomenon investigated in the experimental area.

***Corresponding Author:** R. Soranam ✉ soranamr@gmail.com

INTRODUCTION

When numerous industries produce garbage that seriously pollutes the environment, environmental protection becomes a challenging undertaking. Large amounts of aqueous wastes and dye effluents with high BOD loading and strong, lasting color are released from the dyeing process in the textile sector, which is unsatisfactory from an aesthetic and environmental standpoint (Annadurai and Krishnan, 1997). Aquatic life is seriously at risk because the majorities of these dye wastes are poisonous and may cause cancer (Vandevere *et al*., 1998). Consequently, the elimination of dyestuffs from effluents becomes crucial, and numerous governments have imposed environmental regulations concerning the quality of colored effluents and mandated that enterprises that use dyes decolorize their effluents before to discharge. Numerous conventional dye removal treatment systems, including trickling filters, activated sludge, chemical coagulation, carbon adsorption, and photodegradation processes, have been thoroughly studied (Vandevere *et al*., 1998; Ganesh *et al*., 1994; Gan Yang *et al*., 2008). Among these chemical and physical techniques, the adsorption process is reasonably successful in producing a high-quality effluent without the production of hazardous compounds like ozone and free radicals during the UV photodegradation process.

Activated carbon (Walker and Weatherley, 1997), peat (Poots *et al*., 1976a;1976b; Ho and Mckay, 1998), pith (Mckay *et al*., 1987; Namasivayam *et al*., 1998; Ho and Mckay, 1999; Namasivayam *et al*., 2001; Namasivayam *et al*., 2002), fuller's earth (Atun *et al*., 2003; Mckay *et al*., 1985), and wood (Poots *et al*., 1976a;1976b; Asfour *et al*., 1985). The potential uses of polymeric nanoparticles in medicine and nanotechnological devices, especially as drug delivery vehicles, have drawn more interest in recent years. These nanoparticles are manufactured with a regulated composition, unique supramolecular structures, and dimensions. Due to intra- and or intermolecular interactions of hydrophobic segments in aqueous media, these polymeric nanoparticles with hydrophilic and hydrophobic segments have special properties, including thermodynamic stability, unusual rheological features, and the structure of a hydrophilic shell and a hydrophobic core (Chu and Tsui, 1999; El-Geundi, 1991; Grau, 1991). Polymeric amphiphiles have been thoroughly investigated and identified as promising medication and gene delivery vehicles due to their ability to decrease harmful side effects and enhance therapeutic outcomes. Preparing biodegradable and nontoxic polymeric amphiphiles based on natural biomaterials like chitosan has received a lot of attention lately.

Chitin is deacetylated to generate chitosan, a heteropolymer comprising β - [1→4]-2-amino-2-deoxy-D-glucopyranose and β - [1→4]-2-acetamido-2-deoxy-D-glucopyranose. An essential part of the adsorption process is chitosan; a type of natural polysaccharide made from chitin. The b (1-4)-2-amino-2-deoxy-D-glucopyranose (D-glucosamine) repeating unit makes up the majority of chitosan, a polysaccharide that also contains trace amounts (less than 20%) of N-acetyl-D glucosamine residues (Ali Aberoumand and Maryam Hosseinian, 2025). The polymer has a very high affinity for a variety of dye classes, including disperse, direct, reactive, and acid dyes. It is also non-toxic and biodegradable. Through electrostatic attraction, cationized amino groups can adsorb anionic dye molecules in an acidic aqueous media. The manufacture of chitosan from crab shells is the subject of the proposed study (Musmade and Lalit Mahatma Ali Aberoumand, 2021). The purpose of this research is to achieve the best removal efficiency of methylene blue with short contact and settling durations. Chitosan has been well examined for its capacity to remove dye from textile wastewater effluent. Experiments on a bench scale were carried out to investigate the impact of temperature and pH. Because of its vast surface area, the chitosan is thought to have a greater capacity. The sorption behavior of the chitosan research will be examined (Anggraeni *et al*., 2024).

MATERIALS AND METHODS

Chemicals, reagents, and media

Crab shells were gathered from the fish market and extensively cleaned with distilled water to get rid of any

water-soluble compounds and adherent particles. After that, it was exposed to sunlight for four to five days to dry. The following compounds were graded analytically. Methylene blue, double-distilled water, and acetic acid glacial (CH_3COOH) 100% GR (Merck) were supplied by Merck.

Preparation of chitosan

To the treatment conditions, chitin extraction from prawn and crab shells was accomplished using an alkali-acid treatment, as previously described for other crustacean shells. Samples (also known as crab shells, demineralized, or decolorized samples) were deproteinized by treating them with 1.2 N sodium hydroxide for 2.5 hours at 70-75 °C (10 mL g-1 of samples), demineralized at room temperature with 0.7 N hydrochloric acid (10 mL g-1 of samples) for 15 minutes, and decolorized with acetone for 10 minutes. They were then dried for two hours under a hood, and finally bleached with a 0.32 percent (v/v) solution of sodium hydroxide (10 mL g-1 of samples) for 15 minutes at room temperature. Following each stage, the solid was filtered out and neutralized with distilled water. Chitin deacetylation was performed for 15 minutes at 15 psi/121 °C using a 50% sodium hydroxide solution (13 mL g-1 of chitin). Following this stage, samples were filtered, cleaned with distilled water to achieve a neutral pH, and dried for eight hours at 60 °C in an oven to obtain the commercial chitosan material.

Batch equilibrium studies

The necessary quantities of methylene blue dye were achieved by dissolving the dye in deionized water. The chitosan 0.1 g of adsorbent with different dye concentration at various temperatures (30, 45, and 60°C) and pH levels (5.5, 6.2, and 7.8) was shaken for 24 hours using a water bath to maintain the equilibrium adsorption isotherm tests. The solutions were examined using a UV/Visible spectrometer at the wavelength corresponding to the maximum absorbance (λ_{max}) in order to assess the residual concentrations.

Batch kinetic study

The adsorbent material chitosan (0.1g/L) was added to 100 ml of dye solution (100 mg/L) while stirring continuously. Among the various parameters examined were (i). Effects of dye concentration at constant temperature (30°C) and pH (6.2): 20, 40, and 60 mg/L. (ii). Temperature effects at constant pH (6.2): 30°C, 45°C, and 60°C. (iii). Impact of pH: 5.5, 6.2, and 7.8 at 30°C. The concentrations of dyes were measured with an UV/visible spectrometer was used to measure the dye concentrations. Every experiment was at least repeated under the same circumstances. The following is the quantity of adsorption at time t, qt (mg/g) was obtained as follows;

$$q_t = (C_0 - C_t)/M \quad (1)$$

Where C_0 (mg/L) and C_t (mg/g) are the liquid-phase concentrations of solutes at initial and any time *t*, respectively, M is the dosage of adsorbent in the solution (g/L).

Box-Behnken experiments

The Box-Behnken design was used to maximize the range of testing. Temperature (30, 45, 60 °C) X_1, pH (5.2, 6.2, 7.2) X_2 and time (mints) (20, 60, 140) X_3 were measured. As seen in Table 3, these were the crucial variables for the real studies. A known weight of chitosan (0.1g/L) was added to a 250 ml flask for each experimental batch, and the flask was then incubated for 24 hours at 30 °C on an orbital shaker (150 rpm).

RESULTS AND DISCUSSION

Effect of pH

Fig. 1. shows the dye adsorption on chitosan at various pH values (5.5, 6.2, 7.8). Although there have been various attempts to calculate the amount adsorbed, the most popular method of getting an adsorption isotherm is to measure the concentration of dye solution before and after the adsorption tests (Bravo-Osuna *et al.*, 2010; Cafaggi *et al.*, 2007). The effect of the initial pH for the dye solution was experimentally investigated under a pH range from 5.5 to 7.8 and the results can be observed in Fig. 1. Using chitosan powder, the solution pH has a major effect on chitosan adsorption behavior. It reaches its maximum adsorption efficiency of 17.2mg/g under acidic conditions (pH= 6.2) in comparison with a

12.2mg/g adsorption efficiency under alkaline conditions (pH = 7.8) (Akbar Bayat *et al.*, 2008). The experiments were conducted under the following conditions; temperature 30°C, mixing speed 120 rpm, dose 0.1 g/L, and contact time 60 min (Dan Du *et al.*, 2009).

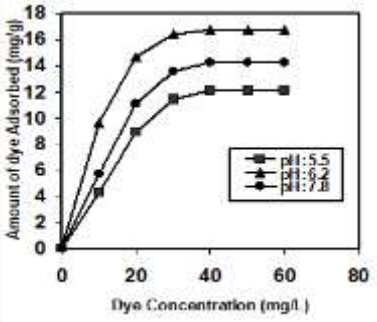

Fig. 1. Effect of specific dye uptake at different pH with dye concentration

Effect of temperature

Fig. 2 illustrates how temperature affects the adsorption of Methylene Blue dye using 20 to 100 mg/L dye solution supplemented with 0.1 g/L of adsorbent dosage under various temperature conditions. Temperature is a crucial parameter that can be regarded as a significant factor in the adsorption process. Between 30 and 60°C, the rate of decolorization rises with temperature. This demonstrates that the process of adsorption is exothermic. According to Le-Chatelier's Principle, adsorption occurs more quickly at lower temperatures and decreases as the temperature rises (Moradi *et al.*, 3009; Karam *et al.*, 2024). The amount of Methylene blue dye absorbed reduces as the temperature rises, demonstrating that the adsorption process generates exothermic heat (Fig. 2). As the temperature rises, the Vander Waals force between the molecules of methylene blue dye and the active sites on the surface of the adsorbent doubles. At higher temperatures, the solvent is more attracted to the surfaces active sites, decreasing the surfaces capacity to adsorb material (Moradi *et al.*, 2009; Ahmad *et al.*, 2021; Karam *et al.*, 2024). As the temperature rises, so does the unpredictable nature of the dye molecules stick to the compounds surface. The adsorption process is also influenced by the surfaces porosity.

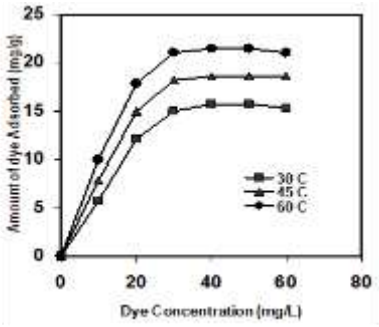

Fig. 2. Effect of specific dye uptake at different temperatures dye concentration

Langmuir isotherm

The adsorption systems, it is crucial to take into account the shape of the adsorption isothermal curve in Fig. 3-4, since it offers insights into the equilibrium curve and other associated phenomena. Based on their main slope, the equilibrium curves are separated into with subgroups distinguished by slope changes and upper section shapes. According to Eteba *et al.* (2022), these groups' L type curves are isotherms of constant partition. The fundamental idea behind the equilibrium curve initial shape (L shape) in Fig. 2 is that, up until the number of adsorption sites cleared is restricted, the higher the solute concentration, the greater the adsorption capacity, leading to competition between solute molecules for the available sites. This form of isotherm states that relatively weak forces, like "van der Waals forces," are responsible for adsorption. The Freundlich and Langmuir isotherms, two significant isotherms, were selected for this investigation from a variety of isothermal models. The Langmuir isotherm has found successful application to many other real sorption processes and it can be used to explain the sorption of dye into chitosan. A basic assumption of the Langmuir theory is that sorption takes place at specific sites within the adsorbent (Poots *et al.*, 1976a; 1976b; Asfour *et al.*, 1985; Fu Chen *et al.*, 2008). The data obtained from the adsorption experiment conducted in the present investigation was fitted in different pH and temperature in isotherm equation. The saturation monolayer can be represented by the expression. The Langmuir isotherm has been effectively used in a number of sorption processes and maintains that sorption takes place at many

homogenous sites inside the adsorbent. The physical simplicity of the isotherm is predicated on the following: (1) adsorption is limited to monolayer coverage. (2) Only one adsorbate molecule can fit in each location. (3) The surface is homogeneous and all places have equal energy

$$q_e = \frac{KbC_e}{(1+bC_e)} \quad (2)$$

$$\frac{1}{q_e} = \frac{1}{K} + \frac{1}{KbC_e} \quad (3)$$

A plot of ($1/q_e$ vs $1/C_e$) resulted in a linear graphical relation indicating the applicability of the above model as shown in (Fig.3-4). The values are calculated from the slope and intercept of different straight line representing the different particle size, pH and temperature (b) energy of adsorption and (k) adsorption capacity and Q_o is represented by (K). The Langmuir isotherm constant (Q_o) in eqn (2-3) is a measure of the amount of dye adsorbed, when the monolayer is completed. Monolayer capacity (Q_o) of the adsorbent for the dye is comparable obtained form adsorption isotherm. The observed statistically significant (at the 95% confidence level) linear relationship as evidenced of these by the R^2 values (close to unity) indicate the applicability of the isotherm (Langmuir isotherm) and surface.

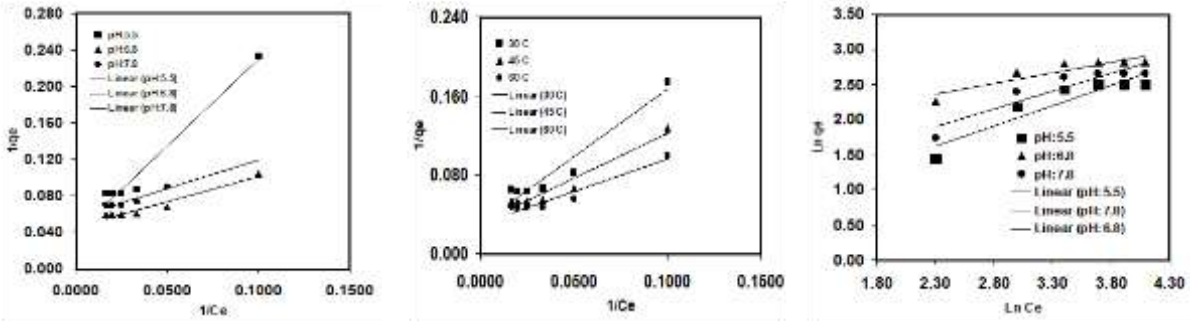

Fig. 3. Langmuir isotherm for the adsorption of dye using Chitosan at different pH with dye concentration

Fig. 4. Langmuir isotherm for the adsorption of dye using Chitosan at different temp. with dye concentration

Fig. 5. Freundlich isotherm for the adsorption of dye using Chitosan at different pH with dye concentration

Freundlich isotherm

Freundlich isotherm is used for heterogeneous surface energies system. The sorption isotherm is the most convenient form of representing the experimental data at different particle sizes, pH and temperature as shown in (Fig. 5-6.). Fig. 5 and 6 show the batch isothermal data fitted to the linear form of the Freundlich isotherm (Ho and Mckay, 1999; Namasivayam *et al.*, 2001; Namasivayam *et al.*, 2002; Atun *et al.*, 2003; Mckay *et al.*, 1985). According to the Freundlich isotherm, adsorption takes place on a heterogeneous surface, and as concentration rises, the adsorbed mass grows exponentially capacity is not assumed to be monolayer as this isotherm describes equilibrium on diverse surfaces. This isotherm in the liquid phase is provided by Equation.

$$q_e = K_F C_e^{1/n} \quad (4)$$

$$\ln q_e = \ln K_F / (1/n) \ln C_e \quad (5)$$

The various constants, associated with the isotherm are the intercept, which is roughly on indicator of sorption capacity (k_f) and the slope (1/n) sorption intensity values are recorded in (Table 1). Freundlich of isotherm has been illustrated to be a special case of heterogeneous surface energies and it can be easily extended to this case. It has been stated by (Fu Chen *et al.*, 2008; Xu-Bio Yuan *et al.*, 2008) that magnitude of the exponent 1/n gives an indication of the favorability and capacity of the adsorbent/adsorbate system.

Adsorption kinetics

The kinetic experiments were carried out by extracting and evaluating the samples at intervals of varying time

(min) till the successive residue dye concentrations became closer in order to comprehend the mechanism of the adsorption process. The well-known kinetic models, the pseudo-first-order model and the pseudo-second-order model, were used to analyze the kinetic data for the adsorption process of methylene dye onto chitosan with an initial dye concentration of 20 mg/L. The kinetics of adsorption was studied for its possible importance in the treatment of dye-containing industrial effluents. Numerous kinetic models have been proposed to elucidate the mechanism by which pollutants are adsorbed at different dye concentration (20, 40, 60 mg/L), pH (5.8, 6.2, 7.8) and temperature (30 45, 60 ^{o}C) as shown in Fig. 7-9.

Table 1. Langmuir and Freundlich isotherm constants at different pH and Temperature

pH	Langmuir Isotherm -model parameters	Freundlich Isotherm -model parameters
5.5	K= 18.53; b= 1.40; R^2= 0.9915	KF = 1.26; n= 0.793; R^2= 0.8433
6.2	K= 86.93; b= 0.82; R2= 0.9456	KF = 1.24; n= 0.795; R^2= 0.8615
7.8	K= 257.37; b= 0.90; R^2= 0.9359	KF= 0.654; n= 1.52; R^2= 0.8712
Temp. (°C)	Langmuir Isotherm -model parameters	Freundlich Isotherm -model parameters
30	K= 18.53; b=1.32; R2=0.9964	KF = 0.912; n= 1.095; R^2= 0.8448
45	K= 86.93; b=0.71; R^2=0.9939	KF = 0.894; n= 1.118; R^2= 0.9332
60	K= 245.0; b= 0.69; R^2=0.9930	KF =0.633; n= 1.579; R^2= 0.9283

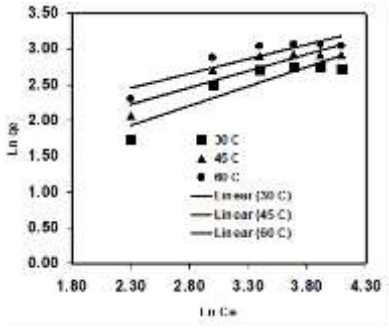

Fig. 6. Freundlich isotherm for the adsorption of dye using Chitosan at different temp.

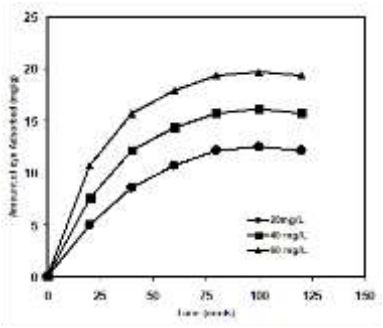

Fig. 7. Effect of specific dye uptake at different dye concentration with time (mints)

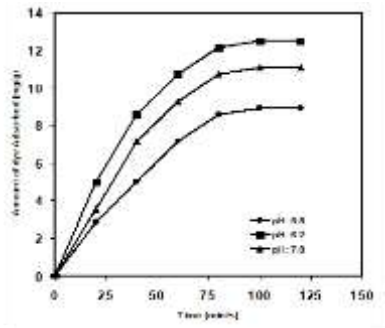

Fig. 8. Effect of specific dye uptake with at different pH with time (mints)

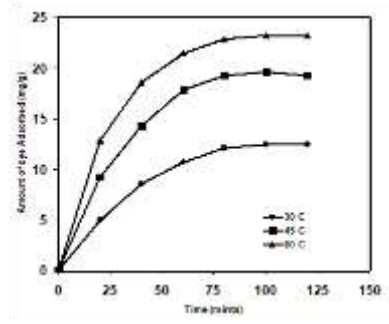

Fig. 9. Effect of specific dye uptake at different temperature with time (mints)

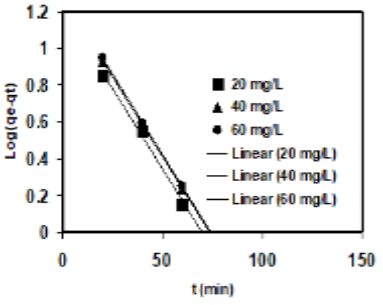

Fig. 10. Pseudo-first order plot for the adsorption of dye using Chitosan at various plot at dye concentration

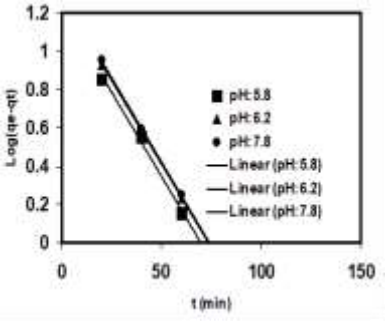

Fig. 11. Pseudo-first order plot for the adsorption of dye using Chitosan at various plot at pH

The large number and array of different chemical groups on chitosan chains (e.g., –NH_2, –OH) imply that there are many types of chitosan–solute interactions (Ho and Mckay, 1999; Namasivayam *et al.*, 2001; Namasivayam *et al.*, 2002; Atun *et al.*, 2003). It is probable that any kinetic or mass transfer representation is likely to be global. From a system design viewpoint, a lumped analysis of adsorption rates is thus sufficient to practical operation. A simple kinetic analysis of adsorption is the pseudo-first-order equation;

$$\frac{dq_t}{q_t} = K_1(q_{eq} - q_t) \quad (6)$$

After definite integration by applying the initial conditions q_t=0 at t=0 and q_t=q_t at t=t, equation (7) becomes;

$$\log(q_{eq} - q_t) = \log q_{eq} - \frac{K_1}{2.303}t \quad (7)$$

Where q_{eq} and q_t are amount of dye adsorbed at equilibrium and at time, in mg g-1 respectively, and K_1 is the first order rate constant, was applied to the present studies of dye adsorption. As such the values of log (q_e-q_t) vs t were calculated form the kinetic data of (Fig. 10-12) and plotted against time. The first-order rate constant calculated form the plots are shown in (Table 2). Adsorption kinetics for some system can also be described by a pseudo-second order reaction (Namasivayam *et al.*, 2002; Atun *et al.*, 2003; Mckay *et al.*, 1985; Poots *et al.*, 1976a; 1976b).

Table 2. Pseudo-first and pseudo-second order rate constant at different dye concentration, pH and temperature

Dye concentration (mg/L)	Pseudo-first order rate constant	Pseudo-second order rate constant
20	K_1=3.354; q_{eq}= 1.41; R^2= 0.9936	K_2=0.0046; q_{eq}=14.02; R^2= 0.9709
40	K_1= 3.36; q_{eq}= 1.54; R^2= 0.9999	K_2= 0.005; q_{eq}=21.08; R^2= 0.9807
60	K_1= 1.29; q_{eq}= 1.45; R^2= 0.9999	K_2=0.0051; q_{eq}= 17.48; R^2=0.9896
pH	Pseudo-first order rate constant	Pseudo-Second order rate constant
5.8	K_1= 0.0653; q_{eq}=1.416; R^2= 0.99363	K_2= 0.0015; q_{eq}=16.07; R^2= 0.8709
6.2	K_1= 0.059; q_{eq}= 1.54; R^2= 0.9999	K_2= 0.0014; q_{eq}= 13.81; R^2= 0.8283
7.8	K_1= 0.10523 q_{eq}= 1.45; R^2= 0.9990	K_2= 0.0018; q_{eq}= 13.87; R^2= 0.9896
Temperature (°C)	Pseudo-first order rate constant	Pseudo-Second order rate constant
30	K_1= 0.0403; q_{eq}= 1.54; R^2= 0.9936	K_2= 0.0105; q_{eq}=13.86; R^2= 0.8293
45	K_1= 0.051; q_{eq}= 1.457; R^2= 0.9999	K_2= 0.006; q_{eq}= 10.42; R^2= 0.7747
60	K_1=0.0136q_{eq}=1.459.10; R^2= 0.9741	K_2= 0.008; q_{eq}= 10.8; R^2= 0.7738

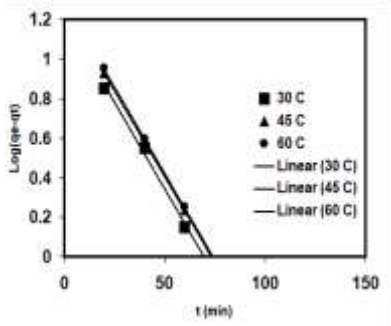

Fig. 12. Pseudo-first order plot for the adsorption of dye using Chitosan at various plot at temperatures

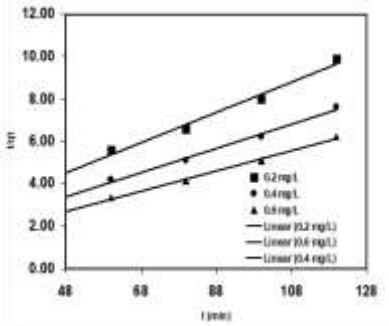

Fig. 13. Pseudo-second order plot for the adsorption of dye using Chitosan at various plot at dye concentration

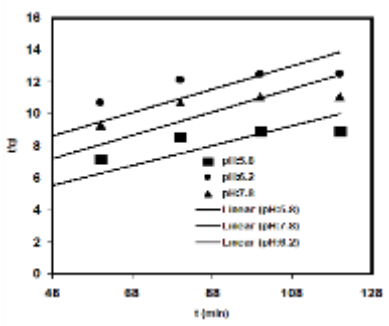

Fig. 14. Pseudo-second order plot for the adsorption of dye Chitosan at various plot at pH

The pseudo-second-order equation based on adsorption equilibrium capacity may be expressed in the form;

$$\frac{dq_t}{q_t} = K_2(q_{eq} - q_t)^2 \quad (8)$$

Where k_2 is the rate constant of pseudo-second-order adsorption. Integrating equation (9) and applying the initial conditions, we have

$$\frac{1}{(q_{eq} - q_t)} = \frac{1}{q_e} + K_2 t \quad (9)$$

or equivalently,

$$\frac{t}{q_t} = \frac{1}{K_2 q_{eq}^2} + \frac{1}{q_e}t \quad (10)$$

The equilibrium adsorption capacity (q_{eq}), and the second-order constants k_2 (g/mg min) can be determined experimentally from the slope and intercept of plot t/q_t versus t.

The applicability of the pseudo-second order models can be examined by linear plot t/q vs t respectively as shown in (Fig. 13-15). The correlation coefficient R^2 shows that the pseudo-second order model an indication of a chemisorption mechanism, fits the experimental data slightly better than the pseudo-first order model. Therefore, the adsorption of methylene blue dye can be approximated more favorably by the pseudo-second order model. This model has been successfully applied to describe the kinetics of many adsorption systems. Calculated correlations are closer to unity for second-order kinetics model; therefore, the adsorption kinetics could well be approximated more favourably by second-order kinetic model for dye adsorption. The k_2 (mg g^{-1} min^{-1}) and q_{eq} (mg g^{-1} min^{-1}) values as calculated are listed in (Table 2).

Design of experimental procedure

Response surface methodology is an empirical modeling technique designed to evaluate the relationship between a set of controlled experimental factors and the observed results. Prior knowledge of the process is required to formulate a statistical model (Box and Hunter, 1957; Box and Behnken, 1960; Cochran and Cox, 1968). Basically, the optimization process involves three major steps: performing the statistically designed experiments; estimating the coefficients in a mathematical model; predicting the response and checking the adequacy of the model.

$$Y = f(X_1, X_2, X_3 \ldots\ldots\ldots X_k) \quad (11)$$

The true relationship between Y and X_k may be complicated and, in most cases, it is unknown; however, a second-degree quadratic polynomial can be used to represent the function in the range of interest,

$$Y = R_o + \sum_{i=1}^{k} R_i X_i + \sum_{i=1}^{k} R_{ii} X_i^2 + \sum_{i=1,i<j}^{k-1} \sum_{j=2}^{k} R_{ij} X_i X_j + \varepsilon \quad (12)$$

where $X_1, X_2, X_3, X_4, \ldots, X_k$ are the input variables which affect the response; Y, R_0, R_i, R_{ii} and R_{ij} ($i = 1–k$, $j = 1–k$) are the known parameters; and ε is the random error. The parameters values have three levels as follows: pH (5.2, 6.8, 7.2), temperature (30,45, 60 ^oC), Time (mints) (20,60,140). This also enables us to identify significant interactions in the batch studies. In systems involving four significant independent variables X_1, X_2, and X_3 indicate the mathematical relationship of the response of these variables which can be approximated by the following quadratic (second degree) polynomial equation:

$$Y = b_0 + b_1X_1 + b_2X_2 + b_3X_3 + b_{11}X_1^2 + b_{22}X_2^2 + b_{33}X_3^3 + b_{12}X_1X_2 + b_{23}X_2X_3 + b_{31}X_3X_1 \quad (13)$$

Where Y is the Predicted value; b_o is a constant; X_1 is the pH; X_2 is the temperature; X_3 is the Time (mints); b_1, b_2, and b_3 are linear coefficients; b_{12}, b_{23}, and b_{31}, are cross product coefficients; and b_{11}, b_{22}, and b_{33} are quadratic coefficients. The critical variables or parameters are chosen and designated X_1, X_2, and X_3. The low, middle and high levels of each variable are designated as -1, 0, and +1, respectively, as seen in Table 3. A total of 17 treatments were necessary to estimate the coefficients of the model using multiple linear regressions. The experimental analysis was carried out using the design expert by Stat Ease lnc (Statistics Made Easy, Minneapolis, MN Version .7).

The regression equation obtained after analysis of the variance gives the level of adsorption of dyes on pH (5.2, 6.8, 7.2), temperature (30,45, 60 ^oC), Time (mints) (20,60,140). A regression model containing 3 linear (X_1, X_2, X_3), 3 quadratic (X_1^2, X_2^2, X_3^2) and 3 interaction (X_1X_2, X_2X_3, X_1X_3) terms, plus 1 block term was employed using the DESIGN EXPERT version (5.7.0.1.1997). The experimental results were analyzed through RSM to obtain find an empirical model for the best response. The theoretically predicted responses are shown in Table.3. The estimated responses seem to have a functional relationship only in or near a local region at the central point of the model. The quadratic model was used to explain the mathematical relationship between the independent variables and the dependent responses.

Table 3. The Box–Behnken design for the three independent variables adsorption dye in actual and predicted values

Run no.	pH X_1	Temperature (°C) X_2	Time (mints) X_3	Experimental value (mg/g)	Predicted value (mg/g)
1	5.2	30	80	15.86	15.99
2	7.2	30	80	16.19	15.81
3	5.2	60	80	15.41	15.79
4	7.2	60	80	17.54	17.41
5	5.2	45	20	16.50	16.38
6	7.2	45	20	16.18	16.55
7	5.2	45	140	18.43	18.05
8	7.2	45	140	19.20	19.33
9	6.2	30	20	16.34	16.34
10	6.2	60	20	17.49	17.24
11	6.2	30	140	18.51	18.76
12	6.2	60	140	19.26	19.26
13	6.2	45	80	22.40	22.40
14	6.2	45	80	22.40	22.40
15	6.2	45	80	22.40	22.40
16	6.2	45	80	22.40	22.40
17	6.2	45	80	22.40	22.40

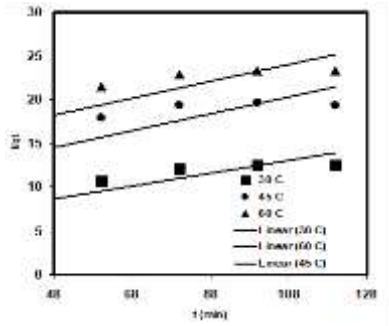

Fig. 15. Pseudo-second order plot for the adsorption of dye using Chitosan at various temperatures

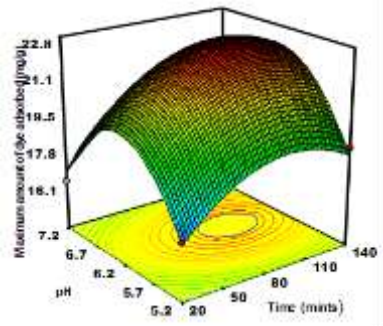

Fig. 16. Adsorption of dye on 3D graphics for response surface optimization versus time (mints) vs pH

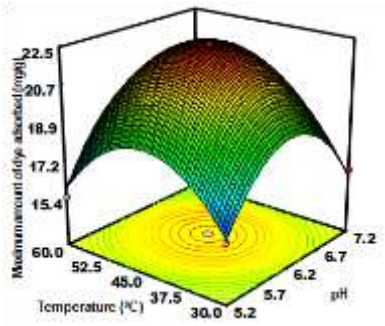

Fig. 17. Adsorption of dye on 3D graphics for response surface optimization versus temperature (°C) vs pH

The mathematical expression of the relationship of the adsorption of dye concentration, pH, and Time (mints) is shown below as coded factors. All terms regardless of their significance are included in the following equation:

$$Y = 22.4 + 0.36X_1 + 0.35X_2 + 1.11X_3 + 3.23X_1^2 + 2.91X_2^2 - 1.58X_3^3 + 0.45X_1X_2 + 0.275X_1X_3 - 0.1X_2X_3 \quad (14)$$

The results of variance analysis (ANOVA) are shown in Table 4. The predictability of the model is at the 99% confidence interval. The predicted response fits the experimentally obtained response well. The coefficient of determination (R^2) value is 0.9934 which shows that the equation is very reliable. A 'p' value of less than 0.0001 indicates that the model is statistically significant. The model was found to be adequate for prediction given the range of variables chosen. Fig. 16-18 shows the observed adsorption of dye versus the values predicted by the statistical model (Eq. 14). The figure makes it clear that the predicted response from the empirical model is in good agreement with the experimentally obtained data.

Effect of pH

The effect of pH on adsorption process was studied at different pH values, namely, 6.7, 8, 5 and 9.5. The results are represented in (Fig. 16). This may be due to the number of positive charges on the sorbent surface which leads to the no rejection of the negatively charged dye molecule, and thereby

increasing the adsorption. In general, the uptakes are much higher in acidic solutions than those in neutral and alkaline conditions. The dye absorption may also derive support from the ion exchange reaction. According to Yoshida (Sanjay K. Motwani *et al.*, 2009; Yujun Wang *et al.*, 2009; Yujun Wang *et al.*, 2009a; 2009b) at lower pH more protons will be available to protonate amine groups of chitosan molecules to form groups $–NH_3^+$, thereby increasing electrostatic attractions between negatively charged dye anions and positively charged adsorption sites and causing an increase in dye adsorption. This explanation agrees with our data on pH effect. It can be seen that the pH of aqueous solution plays an important role in the adsorption of methylene blue onto chitosan (Mckay *et al.*, 1987). All amino groups of the chitosan fibers are cationized and the dye anion pulled in strongly by electrostatic attraction (Gui-yin Li *et al.*, 2009; Gui-yin Li *et al.*, 2009a;2009b; Sanjay K. Motwani *et al.*, 2009). The similar pH effects were also observed by the adsorption of reactive on cross-linked chitosan fibers (Sanjay K. Motwani *et al.*, 2009) adsorption of RR 189 (reactive dye) on cross-linked chitosan beads (Guogen Liua *et al.*, 2007) and reactive dye (RB2, RB2, RY2, RY86) on cross-linked chitosan beads (Mckay *et al.*, 1987).

Table 4. Regression analysis for the adsorption dye by chitosan nanomaterial for quadratic response surface model fitting (ANOVA)

Source	Coefficient value	Mean square	F-value	Prob > F value
X_0	113.1087	12.56763	117.2979	< 0.0001*
X_1	1.05125	1.05125	9.811667	<0.0166*
X_2	0.98	0.98	9.146667	<0.0193
X_3	9.90125	9.90125	92.41167	< 0.0001*
X_1^2	0.81	0.81	7.56	<0.0285*
X_2^2	0.3025	0.3025	2.823333	0.1368
X_3^2	0.04	0.04	0.373333	0.5605
X_1X_2	44.13224	44.13224	411.9009	< 0.0001*
X_1X_3	35.71645	35.71645	333.3535	< 0.0001*
X_2X_3	10.61118	10.61118	99.03772	< 0.0001*
Residual	0.75	0.107143	R-squared = 0.9934	
Lack of fit	0.75	0.25	Adj R-squared=0.9849	
Pure error	0	0		
Correlation total	113.8587			

*Values of "Prob > F" less than 0.0500 indicate model terms are significant.

Effect of temperature

Temperature is an important parameter for the adsorption process. A plot of the Methylene blue uptake as a function of temperature (30, 45 and 60 °C) is shown in (Fig. 17). The results reveal that the dye uptake increased with increasing temperature at 30°C 56.0 mg/g; 45°C 78.0 mg/g and 60°C 96.0 mg/g). The adsorption of dye at higher temperature was found to be greater compared to that at a lower temperature (Jong-Ho Kim *et al.*, 2008; Lin and Lin, 1993). The curves indicate the strong tendency of the process for monolayer formation (Lucarelli *et al.*, 2000; Poots *et al.*, 1997a;1997b). The increase in temperature would increase the mobility of the large dye ion and also produces a swelling effect with in the internal structure of the chitosan, thus enabling the large dye molecule to penetrate further (Sanjay K. Motwani *et al.*, 2009; Yujun Wang *et al.*, 2009a; 2009b).

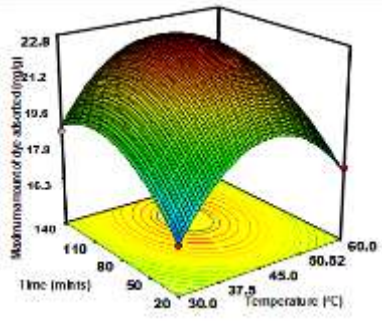

Fig. 18. Adsorption of dye on 3D graphics for response surface optimization versus time (mints) vs temperature (°C)

Therefore, the adsorption capacity should largely depend on the chemical interaction between the

functional groups on the adsorbent surface and the adsorbate and should increase with temperature rising. This can be explained in that an increasing diffusion rate of the adsorbate into the pores of the adsorbent at higher temperature might contribute to the Remazol black 13 (Reactive dye) adsorption, as diffusion is an exothermic process (Guogen Liua *et al.*, 2007; Gui-yin Li *et al.*, 2009).

Effect of time (mints)

The maximum amount of dye adsorption (88.45 to 97.71mg/g) to chitosan can be clearly seen in Fig. 18. The optimal adsorption was 21.2 mg/g with 80.0 time (mints) with Temperature (45^{o}C) and a dye concentration of 40.0mg/L (Rajesh Kumar *et al.*, 2008; Tze-Wen Chunga *et al.*, 2008a;2008b). The most probable explanation for the effect of the mass of orange peel on the biosorption of microbial cells form the bulk solution is that as the mass increased both the available adsorbent surface area and the pore surface area (Yakup Arica, 2001).

CONCLUSION

The purpose of this study is to investigate the ability of a adsorbent made from chitosan (crab shells) to bind dyestuffs. We will look at the potential of employing adsorbent wastewater and Agric-food industrial wastewater treatment plants. (i) Chitin will be prepared from crab and prawn shells at varying concentrations (NaOH); (ii) Chitosan will be prepared by soaking it in sodium hydroxide for 2.5 hours at 70-75 degrees Celsius, demineralizing it at room temperature with 0.7 to 1.0 N hydrochloric acid for 15 minutes, decolorizing it with acetone for 10 minutes, and drying it for 2 hours. Then, it will be bleached with a 0.32% (v/v) solution of sodium hydroxide (containing 5.25% available chlorine) for 15 minutes at room temperature.

Dyestuff will be utilized as an adsorbent to describe the adsorption capacity of various sorbent material conditions. Freundlich was used to examine the experimental isotherm data, and Langmuir was calculated for each isotherm analysis. The equilibrium, pH, and temperature margins of the tests were used to analyze the material sorption behavior. The equilibrium data were fitted using two isotherms (Langmuir and Freundlich). We will look into the surface area that corresponds to chemically sorbent and pyrolyzed materials. The adsorption kinetic data will be interpreted using the kinetic models, namely pseudo-first-order and pseudo-second. The elimination of dyestuff will be modelled mathematically using the Box-Behnken design of trials. Three main processes are anticipated by this optimization method, which involves the coefficients in a mathematical model: carrying out statistically planned experiments, estimating the coefficient in a mathematical model, forecasting the response, and determining the model's adequacy.

ACKNOWLEDGEMENTS

In order to complete this study M. Priyanga (Reg. 22214012052023) appreciates the Sri Paramakalyani Centre for Excellence in Environmental Science at Manonmaniam Sundaranar University in Alwarkurichi, India.

REFERENCES

Ahmad MB, Soomro U, Muqeet M, Ahmed Z. 2021. Adsorption of Indigo Carmine dye onto the surface modified adsorbent prepared from municipal waste and simulation using deep neural network. J Hazard Mater **408**, 1244.

Akbar Bayat F, Dorkoosh A, Ahmad Reza D, Leila M, Bagher L, Hans E. Junginger, MR. 2008. Nanoparticles of quaternized chitosan derivatives as a carrier for colon delivery of insulin: Ex vivo and in vivo studies International Journal of Pharmaceutics **356** (22), 259-266.

Ali Aberoumand, Maryam Hosseinian. 2025. Extraction of Chitosan from shells of crab (*Liocarcinus vernalis*). Applied Food Research **5**(1), 100964.

Anggraeni AS, Jayanegara A, Laconi EB. Kumalasari NR, Windarsih A, Sofyan A. 2024. Physicochemical and antibacterial properties of chitosan extracted from swimming crab shells and wooden grasshoppers using different extraction methods. Food Research **8**(3), 439 – 450.

Annadurai G, Krishnan MRV. 1997. Batch equilibrium adsorption of reactive dye onto natural biopolymer. Iran Polym. J**. 6**, 169-175.

Asfour HM, Nassar MM, Fadali OA, Elgeundi MS. 1985. Colour removal from textile effluents using hardwood sawdust as an absorbent. J Chem Technol Biotechnol. **35**, 28-35.

Atun G, Hisarli G, Sheldrick WS, Muhler M. 2003. Equilibrium Studies for Acid Dye Adsorption onto Chitosan. J Colloid Interface Sci. **261**, 32-39.

Box GEP, Hunter JS. 1957. Multi-Factor Experimental Designs for Exploring Response Surfaces. The Annals of Mathematical Statistics **28**, 195-241.

Box GEP, Behnken DW, 1960. Some New Three Level Designs for the Study of Quantitative Variables. Technometrics **2**, 455-475.

Bravo-Osuna C, Vauthier Chacun H, Ponchel G. 2009. Surface-functionalized polymethacrylic acid-based hydrogel microparticles for oral drug delivery. European Journal of Pharmaceutics and Biopharmaceutics **74**, 209-2018.

Cafaggi S, Russo E, Stefani R, Leardia R, Cavigliolia G. Parodi B, Bignardi G, De Totero D, Aiello C, Viale M. 2007. Controlled release of biomolecules from temperature-sensitive hydrogels prepared by radiation polymerization. Journal of Controlled Release **75**(1-2), 173-81.

Chu W, Tsui SM. 1999. Bisphenol A in hazardous waste landfill leachates. Chemosphere **39,** 1667-16677.

Cochran WG, Cox DW. 1968. Experimental design, John Wiley and Sons, Inc, New York. 611-626.

Dan Du, Shizhen Chena, Jie Cai, Dandan Song. 2009. Comparison of drug sensitivity using acetylcholinesterase biosensor based on nanoparticles-chitosan sol–gel composite. Journal of Electroanalytical Chemistry **611,** 60-66.

El-Geundi MS. 1991. Preparation of a macroporous silica-based multidentate soft-ligand material and its application in the adsorption of palladium and the others. Water Res. **25**, 271e3.

Eteba A, Bassyouni M, Saleh, M. 2022. Modified coal fly ash for textile dye removal from industrial wastewater. Energy Environ. **35**(2), 1-7, 2022.

Fu Chen, Zhi-Rong Zhang, Fang Yuan, Xuan Qin, Minting Wang, Yuan. 2008. *In vitro* and *in vivo* study of *N*-trimethyl chitosan nanoparticles for oral protein delivery. Huang International Journal of Pharmaceutics **349**, 226–233.2008.

Gan Yang, Ruo Yuan, Ya-Qin Chai. 2008. A high-sensitive amperometric hydrogen peroxide biosensor based on the immobilization of hemoglobin on gold colloid/l-cysteine/gold colloid/nanoparticles Pt–chitosan composite film-modified platinum disk electrode. Colloids and Surfaces B: Biointerfaces **61**, 2008, 93–100.

Ganesh R, Boardman GD, Michelsen D. 1997. Color removal of real textile wastewater by sequential anaerobic and aerobic reactors. Water Res. **28**, 1367-1376.

Grau P. 1991. Textile industry wastewaters treatment. Water Sci Technol. **24**, 97-103.

Gui-yin Li, Yu-ren Jiang, Ke-long Huang, Ping Ding, Jie Chen. 2009a. Preparation and properties of magnetic Fe_3O_4–chitosan nanoparticles. Journal of Alloys and Compounds **466**(12), 451-456.

Gui-yin Li, Yu-ren Jiang, Ke-long Huang, Ping Ding, Jie Chen. 2009b. Highly selective reduction of nitroarenes by iron nanoparticles in water. Chemical Communication **64,** 2012, 1-7.

Guogen Liua, Lei Shao, Fei Gea, Jianfeng Chen. 2007. Chitosan Microparticulate Systems Prepared By Polymer-Surfactant Interaction China Particuology **5**, 384-390.

Ho YS, McKay G. 1999. A kinetic study of dye sorption by biosorbent waste product pith. Resour Conserv Recy. **25**, 171-193.

Ho YS, McKay G. 1998. Sorption of dye from aqueous solution by peat. Chem Eng J. **70**, 115-124.

Jong-Ho Kim, Yoo-Shin Kim, Kyeongsoon Park, Seulki Lee, Hae Yun Nam, Kyung Hyun Min, Hyung Gon Jo, Jae Hyung Park, Kuiwon Choi, Seo Young Jeong, Rang-Woon Park, In-San Kim, Kwangmeyung Kim, Ick Chan Kwon. 2008. Antitumor efficacy of cisplatin-loaded glycol chitosan nanoparticles in tumor-bearing mice. Journal of Controlled Release **127**(1-7), 41-49.

Karam K, Alwan A, Faiq F. 2024. Adsorption of Indigo Carmine Dye on Chitosan Grafted Poly (Methyl Methacrylate). Baghdad Science Journal **1**, 1-10.

Lin SH, Lin CM. 1993. Treatment of textile waste effluents by ozonation and chemical coagulation, Water Res. **27**, 1743-1748.

Lucarelli L, Nadtochenko V, Kiwi J. 2000. Environmental Photochemistry: Quantitative Adsorption and FTIR Studies during the TiO_2-Photocatalyzed Degradation of Orange II. Langmuir **16**, 102-1108.

McKay G, Elgeundi M, Nassar MM. 1987. Equilibrium studies during the removal of dyestuffs from aqueous solutions using Bagasse pith. Water Res. **21**, 1513-1520.

McKayG, Otterburn MS, Aga JA. 1985. Fuller's earth and fired clay as adsorbents for dyestuffs. Water, Air, and Soil Pollution **24**, 307–322.

Min Lang Tsai, Shi Wei Bai, Rong Huei Chen. 2008. Cavitation effects versus stretch effects resulted in different size and polydispersity of ionotropic gelation chitosan–sodium tripolyphosphate nanoparticle. Carbohydrate Polymers **71,** 448–457.

Ming-Cheng Weia, Hao-Jan Linc, Hsing-Wen Sunga. 2008. The use of biodegradable polymeric nanoparticles in combination with a low-pressure gene gun for transdermal DNA delivery. Biomaterials **29**, 742–751.

Moradi O, Aghaie M, Zare K. 2009. The study of adsorption characteristics Cu^{2+} and Pb^{2+} ions onto PHEMA and P(MMA-HEMA) surfaces from aqueous single solution. J. Hazard. Mater. **170**, 673 –679.

Musmade NA, Lalit Mahatma A. 2025. Maryam Hoseinian Extraction of Chitosan from shells of crab (*Liocarcinus vernalis*). Applied Food Research **5**(1), 100964.

Namasivayam C, Kavitha D. 2002. Removal of Congo Red from water by adsorption onto activated carbon prepared from coir pith, an agricultural solidwaste. Dyes Pigments **54**, 47-58.

Namasivayam C, Prabha D, Kumutha M. 1998. Removal of direct red and acid brilliant blue by adsorption on to banana pith. Bioresource Technol. **64**, 77-79.

Namasivayam C, Radhika R, Suba S. 2201. Preparation of a Macroporous Silica-Based Pyridine Impregnated Material and Its Adsorption for Palladium.Waste Manage. **21**, 381-397.

Poots VJP, McKay G, Healy JJ. 1976. Evaluation of use of fly ash-gypsum mixture for rice production at different nitrogen rates. Water Res. **10**, 106-116.

Poots VJP, McKay G, Healy JJ. 1976. The removal of acid dye from effluent using natural adsorbents—II Wood. Water Res.**76**, 1067-1070.

Rajesh Kumar S, Ishaq Ahmed VP, Parameswaran V, Sudhakaran R, Sarath Babu V, Sahul Hameed AS. 2009. Potential use of chitosan nanoparticles for oral delivery of DNA vaccine in Asian sea bass (*Lates calcarifer*) to protect from *Vibrio* (*Listonella*) *anguillarum*. Fish & Shellfish Immunology **25**, 47-56.

Sanjay K. Motwani, Shruti Chopra, Sushma Talegaonkar, Kanchan Kohli, Farhan J. Ahmad, Roop K. Khar. 2009. Chitosan-sodium alginate nanoparticles as submicroscopic reservoirs for ocular delivery: formulation, optimisation and *in vitro* characterisation. Eur J Pharm Biopharm. **68**(3), 513-25.

Tze-Wen Chunga, Shoei-Shen Wangb, Wei-Jain Tsai. 2008a. Accelerating thrombolysis with chitosan-coated plasminogen activators encapsulated in poly-(lactide-*co*-glycolide) (PLGA) nanoparticles. Biomaterials **29**, 228–237.

Tze-Wen Chunga, Shoei-Shen Wangb, Wei-Jain Tsai. 2008b. Production of chitosan oligosaccharides using chitosanase immobilized on amylose-coated magnetic nanoparticles. Process Biochemistry **43**, 62–69.

Vandevivere PC, Bianchi R, Verstraete W. 1985.nReview: Treatment and reuse of wastewater from the textile wet-processing industry: Review of emerging technologies. Water, Air, Soil Pollut. **24**, 307-322.

Walker GM, Weatherley LR. 1997. Adsorption of acid dyes on to granular activated carbon in fixed beds. Water Res. **31**, 2093-2101.

Xu-Bo Yuan, Yan-Bo Yuan, Wei Jiang, Jie Liua, En-Jiang Tianc, Hui-Ming Shunc, Ding-Hai Huanga, Xiao-Yan Yuan, Hong Lid, Jing Sheng. 2008. Preparation of rapamycin-loaded chitosan/PLA nanoparticles for immunosuppression in corneal transplantation. International Journal of Pharmaceutics **349**, 241–248.

Yakup Arica M , Akin-Oktem G, Denizli A. 2001. Novel hydrophobic ligand-containing hydrogel membrane matrix: preparation and application to gamma-globulins adsorption. Colloids Surf B Biointerfaces **1**(4), 273-283.

Yujun Wang, Xianghua Wang, Guangsheng Luo, Youyuan Dai. 2009a. Adsorption of bovin serum albumin (BSA) onto the magnetic chitosan nanoparticles prepared by a microemulsion system. Bioresource Technology **99**(9), 3881- 3884.

Yujun Wang, Xianghua Wang, Guangsheng Luo, Youyuan Dai. 2009b. *In situ* preparation of magnetic Fe3O4-chitosan nanoparticles for lipase immobilization by cross-linking and oxidation in aqueous solution. Bioresource Technology **100**(14), 3459-64.